

50 COP

FACILITY FORM 802

N65 18148
(ACCESSION NUMBER)

24
(PAGES)

CR-57039
(NASA CR OR TMX OR AD NUMBER)

(THRU)

1

(CODE)

14

(CATEGORY)

Technical Report No. 32-643

*On the Construction and Theory of a Miniature
Stress Transducer to Measure Radial
Stress in Propellant Grains*

*Anthony San Miguel
Robert H. Silver*

GPO PRICE \$ _____

OTS PRICE(S) \$ _____

Hard copy (HC) \$1.00

Microfiche (MF) \$0.50

JET PROPULSION LABORATORY
CALIFORNIA INSTITUTE OF TECHNOLOGY
PASADENA, CALIFORNIA

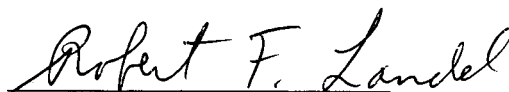
February 15, 1965

Technical Report No. 32-643

*On the Construction and Theory of a Miniature
Stress Transducer to Measure Radial
Stress in Propellant Grains*

Anthony San Miguel

Robert H. Silver

A handwritten signature in cursive script, reading "Robert F. Landel". The signature is written in dark ink and is positioned above a horizontal line.

Robert F. Landel, Chief
Polymer Research Section

JET PROPULSION LABORATORY
CALIFORNIA INSTITUTE OF TECHNOLOGY
PASADENA, CALIFORNIA

February 15, 1965

Copyright © 1965
Jet Propulsion Laboratory
California Institute of Technology

Prepared Under Contract No. NAS 7-100
National Aeronautics & Space Administration

CONTENTS

I. Introduction	1
II. Transducer Nonlinearity	2
A. <i>p</i> -Type Silicon Splinter Nonlinearity	2
B. Circuitry Nonlinearity	4
III. The Stress Transducer	5
IV. Gage Application	14
V. Discussion	16
VI. Conclusion	17
Nomenclature	18
References	18

FIGURES

1. Typical resistance—strain (stress) response of a silicon splinter	3
2. Electromechanical coupling of silicon	3
3. Constant-voltage Wheatstone bridge	4
4. The miniature stress transducer	5
5. A spool-type stress transducer in a tensile bar	6
6. Basic elements of the miniature stress transducer	6
7. A preliminary miniature stress rosette	7
8. The construction aspects of the miniature stress transducer	8
9. Jeweler's lathe and magnifying lenses essential to transducer construction	9
10. Threading and welding phase of transducer construction	9
11. Compression calibration mold	10
12. Tensile calibration mold	10
13. Calibrated response of transducer in compression	10
14. Compression calibration apparatus	11
15. Calibrated response of transducer in tension	12
16. Tensile failure near the miniature stress transducer	12

FIGURES (Cont'd)

17. Stress-rate response of typical transducer	13
18. Transducer-positioning mold	14
19. Positioned transducer in thick-walled cylinder	15
20. Inflated cylinder test	16
21. Experimental vs. theoretical values for radial stress in a pressurized cylinder	17

ABSTRACT

18148

The first of what may truly be called a miniature, directional stress transducer has been developed, constructed, and evaluated at JPL. The transducer discussed in this Report is a device that measures a directional force being experienced within a deformed material, such as a pressurized solid-propellant motor. The transducer has been used to measure a radial stress in a propellant grain. This transducer is 0.100 in. long and 0.046 in. in diameter. The active element is a piezoresistive *p*-type silicon splinter. A 2-mil lead wire transmits signals from the transducer to recording equipment. Complete information is presented regarding the transducer construction. Nonlinearity problems are discussed both from the point of view of the circuitry and of the piezoresistance. Casting techniques for calibrating and embedding the transducer are described. Finally, transducer response vs. grain pressurization is compared with theoretical predictions of radial stress.

**I. INTRODUCTION**

A prerequisite for material property or stress analysis investigations is a knowledge of multiaxial stress distributions within the material being subjected to environmental restraints. Aside from a few experimental techniques, e.g., the use of photoelastic models, little effort has been directed toward measuring the three principal stresses existing in a point region within a material. A perusal of any engineering handbook would give the impression that material properties are based solely on deformation measurements and external loadings.

One reason that little emphasis has been placed on direct stress measurements is that equilibrium conditions, à la stress functions, allow reasonable predictions of stresses in simple geometries. Another reason has been that engineers have been conditioned to working with such materials as wood and metal. These materials

obviously are not conducive to stress transducer embedment. On the other hand, plastics, rubbers, concrete, and solid propellant would seem to be made to order for such devices. Few, if any, attempts have been made to measure stresses within rubber-like materials, although various attempts, some of them successful, have been made to measure deformations within rubber-like materials (Ref. 1, 2, 3).

A distinction must be made between a strain transducer, e.g., a wire strain gage, and a stress transducer, e.g., a load cell. In the former, large deformations must be experienced by the transducer; in the latter, the transducer is characterized by its rigidity. In many instances, the distinction between strain and stress measurement is a moot point. On the other hand, the distinction would be significant when making viscoelasticity measurements,

e.g., in measuring creep. A packaging problem exists for either type of transducer. The function of packaging is to condense or amplify the deformation or force of the surrounding medium to one compatible with the sensing element. An added problem with packaging a transducer to be used in a viscoelastic medium has to do with matching boundary conditions between the packaging material and the surrounding medium.

A feasibility study to develop a direction-oriented miniature stress transducer was first reported in Ref. 4. One transducer developed in this study consisted of a *p*-type [111 orientation] silicon splinter semiconductor packaged in a machined cylinder of Bakelite about 0.130 in. long and 0.050 in. in diameter. This transducer partially satisfied the specifications for a practical stress transducer to be used to measure radial stresses in a solid-propellant grain. Preliminary design specifications were (1) that the stress transducer operate at ambient temperature with repeatability and negligible hysteresis, (2) that it measure a uniaxial compressive stress from

0 to 100 psi in an unrestricted propellant grain, and (3) that the design could feasibly be miniaturized to 0.05 in. in length. This latter dimension was considered small enough to avoid the undesirable effects associated with rigid inclusions.

The physical phenomenon of the sensing element being exploited in this Report is that of piezoresistance (Ref. 5). The problems associated with the nonlinearity inherent in a silicon splinter and a Wheatstone bridge circuit are also reviewed. Three stress transducers were calibrated, both in tension and compression, and inserted at the center (in the radial direction) of three unrestricted cylinders (6-in. OD, 2-in. ID, by 5-in. length) of polyurethane resin (Ref. 6) in order to provide a comparison with results obtained using elasticity theory. These cylinders were pressurized using the inflated cylinder test instrumentation (Ref. 7). The measured radial stress at a point region was then compared with the theoretical radial stress obtained from the classical equations for thick-walled cylinders.

II. TRANSDUCER NONLINEARITY

Nonlinear transducer response can arise from two sources, the splinter itself and/or the electric circuitry. Historically, experimentalists have gone to great extents to obtain linear responses from transducers. However, a nonlinear but repeatable response is not necessarily unsatisfactory, although the final data conversion is complicated. Even though a cause-and-effect response is nonlinear, the phenomenon under investigation can still be resolved. This may be accomplished for many different environments, provided that a calibration has been performed using these different environments and that the same recording instrumentation is employed.

A. *p*-Type Silicon Splinter Nonlinearity

It can be shown (Ref. 8, p. 113) that the resistance-vs.-stress response of a *p*-type silicon splinter oriented in the 111-*k* space can be approximated by an equation of the following form:

$$\frac{\Delta R}{R} = A\tau_{11} + B\tau_{11}^2$$

where the uniaxial strain is

$$S = \frac{\tau_{11}}{E}$$

The constant *B* is negative for low splinter doping, whereas it is positive for high splinter doping. Measurements of a highly doped splinter indicate less nonlinearity between stress and resistance than those of a lightly doped splinter. Nonlinearity can also be introduced by the source current heating the splinter. Hence, a compromise between applied current or voltage and heating (power dissipation) must be made. A linear relationship exists between change in resistance and applied longitudinal stress for splinter strain levels of at least 1000 $\mu\text{in./in.}$ Figure 1 illustrates a typical resistance-strain (stress) response of a silicon splinter (P01-05-120, Micro-Sensor, Micro Systems, Pasadena, Calif.) used in this study. The maximum linear range preferred for the splinter used in this study was between 800 and 1000 $\mu\text{in./in.}$ of compressive strain. In general, the stress-strain curve of a silicon splinter is linear up to its fracture point

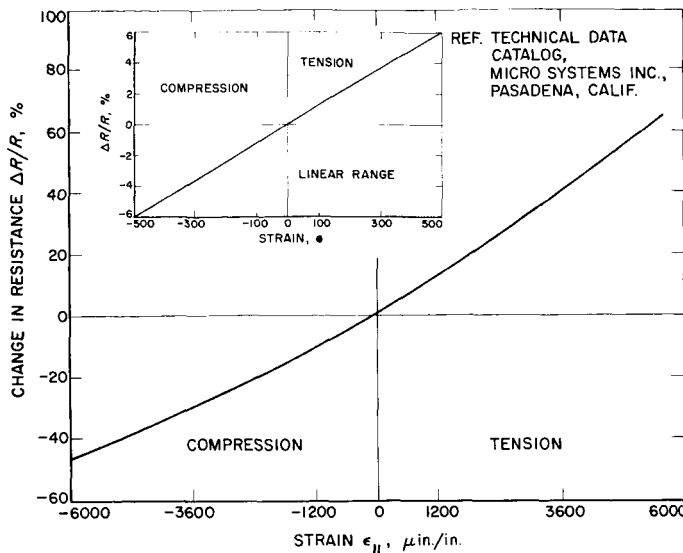


Fig. 1. Typical resistance-strain (stress) response of a silicon splinter

for temperatures of less than 500°C. The Micro Systems Co. representatives state that their splinters have an operative range of $\pm 3000 \mu\text{in./in.}$ strain and imply that many splinters will actually withstand 5000 to 6000 $\mu\text{in./in.}$ strain in tension, and even more in compression. Hence, safe linear operation values should be expected up to 1000 $\mu\text{in./in.}$ strain.

The fact that the Micro Systems silicon splinters are characterized in terms of strain should not be unduly disturbing, since the company's primary product has been in the strain-measuring realm. It will be shown below that the basic physical phenomenon of piezoresistance is associated with *stress* and resistance, not strain and resistance. The anisotropic constitutive relationships between stress and strain would have to be established for silicon before an exact relationship between strain and resistance could be explicitly established.

Based on the observations discussed above, it is completely feasible to linearize the silicon splinter response by

1. Imposing a preload condition via packaging
2. Changing the doping density
3. Changing the applied voltage across the splinter.

These three design variables must be considered in the design of a transducer that is to be employed in any particular stress-measuring experiment.

A silicon splinter exhibits anisotropic piezoresistance, that is, its resistance depends on the applied stress magnitude and direction. Piezoresistance should not be con-

fused with piezoelectricity, the development of a voltage by an applied stress. The theoretical treatment of piezoresistance is analogous to that of classical elasticity. Whether such an analogous treatment is appropriate remains to be seen. On the other hand, the infinitesimal strains experienced by the silicon and the presumed fact that the silicon is indeed linearly elastic (but anisotropic) lend themselves to classical elasticity theory.

It has been assumed in the literature of solid-state physics that the semiconductor property that changes, if a shear stress is applied to silicon, is the ratio of an electric field component to a perpendicular current density component. Referring to Fig. 2, the general constitutive equations for silicon are:

$$\begin{aligned}\frac{E_1}{R_0} &= i_1 [1 + \pi_{11}\tau_{11} + \pi_{12}(\tau_{22} + \tau_{33})] + \pi_{44}(i_2\tau_{12} + i_3\tau_{13}) \\ \frac{E_2}{R_0} &= i_2 [1 + \pi_{11}\tau_{22} + \pi_{12}(\tau_{11} + \tau_{33})] + \pi_{44}(i_1\tau_{12} + i_3\tau_{23}) \\ \frac{E_3}{R_0} &= i_3 [1 + \pi_{11}\tau_{33} + \pi_{12}(\tau_{11} + \tau_{22})] + \pi_{44}(i_1\tau_{13} + i_2\tau_{23})\end{aligned}\quad (2)$$

where E_i = the electric field component

i_i = the current component

$\pi_{11}, \pi_{12}, \pi_{44}$ = piezoresistance coefficients unique to silicon

τ_{ij} = general stress tensor

$R_0 = (\rho l)/A$ = initial electrical resistance of silicon

l = length of splinter

A = cross-sectional area of splinter

ρ = resistivity under zero stress

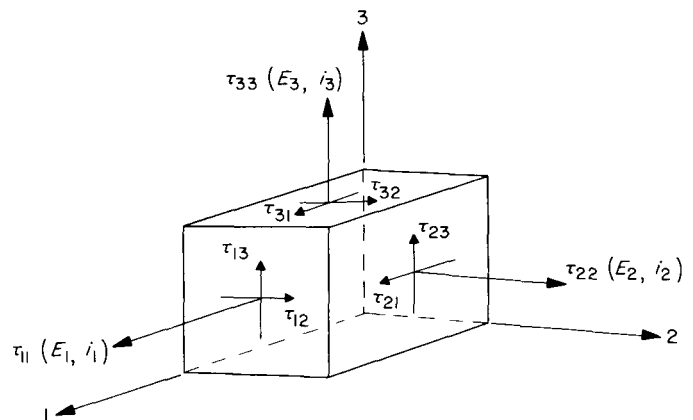


Fig. 2. Electromechanical coupling of silicon

A piezoresistive coefficient, π_l , could presumably be computed along any axis other than the crystallographic axis from the equation

$$\pi_l = \pi_{11} + 2(\pi_{44} + \pi_{12} - \pi_{11})(l_{11}^2 l_{12}^2 + l_{11}^2 l_{13}^2 + l_{12}^2 l_{13}^2) \quad (3)$$

where l_{11}, l_{12}, l_{13} are the direction cosines used in a fashion analogous to the method of finding principal stresses or strains.

The values of the piezoresistance coefficients have reportedly been measured (Ref. 9) and found to be

$$\rho = 11.7 \text{ ohm-cm}$$

$$\pi_{11} = -102.2 \times 10^{-12} \text{ cm}^2/\text{dyne}$$

$$\pi_{12} = 53.4 \times 10^{-12} \text{ cm}^2/\text{dyne}$$

$$\pi_{44} = -13.6 \times 10^{-12} \text{ cm}^2/\text{dyne, or}$$

$$(\pi_l)_{111} = -81.3 \text{ cm}^2/\text{dyne, and}$$

Young's modulus = 1.87×10^{12} dynes/cm² for a *p*-type [111] silicon splinter at room temperature.

These values should be considered only as illustrative, since various lots of silicon splinters will have different values.

The only silicon splinter considered to date at the Jet Propulsion Laboratory has been a [111] orientation in the *k*-crystallographic space. This splinter orientation is readily available commercially because it gives a maximum value of π_l (since $l_{11} = l_{12} = l_{13} = 1/\sqrt{3}$) and is in the most useful orientation for strain-gage applications.

It is apparent from Eq. 2 that nonlinearity can be attributed to neglect of those stress components that are inherent in an arbitrarily loaded medium, which would be a consequence of a general stress field. Thus, it is recognized that Eq. 1 is really a special case of Eq. 2. The point to be made is that Eq. 1 should suffice for exploratory transducer development studies and that Eq. 2 be used as a guide to transducer refinement.

B. Circuitry Nonlinearity

A constant-current circuit would, in theory, be the linear circuit to be used with semiconductor transducers.

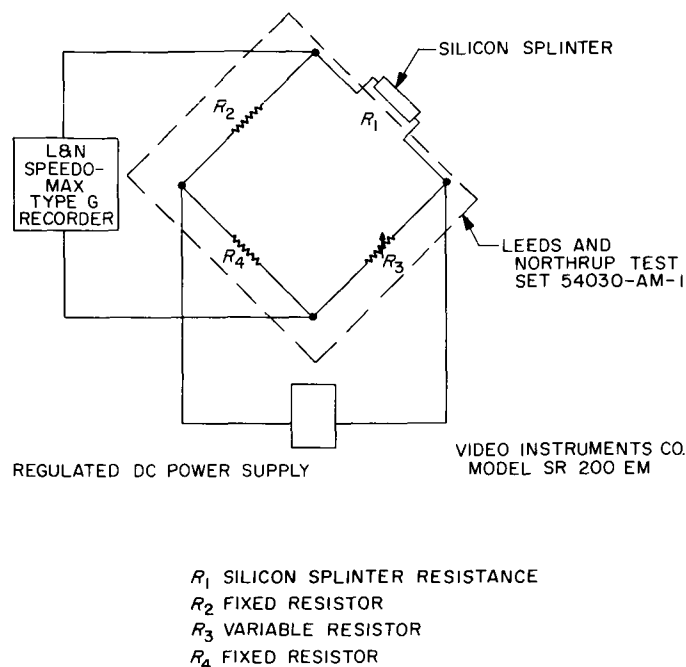


Fig. 3. Constant-voltage Wheatstone bridge

However, a constant-voltage Wheatstone bridge was used to calibrate the transducers being investigated. A schematic of this circuitry is shown in Fig. 3. This circuitry is a reasonable one to use for simple conditions in which high accuracy is not required and in which the temperature is held relatively constant during the calibration. This ordinary Wheatstone bridge was used to measure the resistance change of the transducer that was due to longitudinal load, and the difference in resistance was used to calculate stress.

The instrumentation consisted of a Leeds and Northrup Model 54030-AM-1 Wheatstone Bridge box, to which the transducer was connected across the unknown resistance terminals. A constant voltage supply was connected across the bridge as shown in Fig. 3. The unbalance of the bridge circuit was recorded by means of a Leeds and Northrup Model G 5-mv-full-scale strip chart recorder. The recorder was initially calibrated for zero at the bridge balance condition. As a compressive or tensile stress is applied to the transducer, the resistance R begins to decrease or increase and causes an unbalanced condition in the bridge circuit. The voltage from the bridge circuit, E_o , is recorded on the strip chart recorder.

The output voltage of a Wheatstone bridge circuit at balance, i.e., when $R_1 R_4 = R_2 R_3$, is zero. If one arm,

say R_1 , is changed slightly to $R_1 + \Delta R$, the output voltage is given by

$$E_o = E_{in} \frac{R_4}{(R_1 + R_2)(R_3 + R_4)} \times \frac{\Delta R}{1 + \Delta R/(R_1 + R_2)} \quad (4)$$

It is obvious from this relationship that for a large ΔR , nonlinearity is significant. For equal arms, i.e., when

all R_i are equal, the nonlinearity can be as much as 10% for a 20% change in the resistance of the transducer arm, R_1 . If R_2 and R_4 are made large in comparison with R_1 and R_3 , this nonlinearity is reduced. By proper adjustment of the ratio of R_2 and R_4 with respect to R_1 and R_3 , the nonlinearity of the Wheatstone bridge circuit can be minimized. In the present apparatus, R_1 is the resistance of the unloaded transducer, and ΔR is the change induced on loading.

III. THE STRESS TRANSDUCER

Only one type of miniature unidirectional stress transducer is discussed in this Report (Fig. 4), although various similar types of transducers have been developed (Fig. 5) and are currently being evaluated for multiaxial stress fields (stress rosette).

The philosophy underlying the stress transducer design is to embed a rigid splinter with relatively small strain

(but high stress) capabilities within a strain-condensing package such as etched Teflon (Fig. 6). The strain-reducing medium, e.g., Teflon, condenses a class of propellant strain amplitudes to a level that is compatible with that of the rigid splinter. Ideally, one would want the mechanical properties of the transducer to be the same as those of the surrounding material (propellant). However, this property is not necessary, or even feasible,

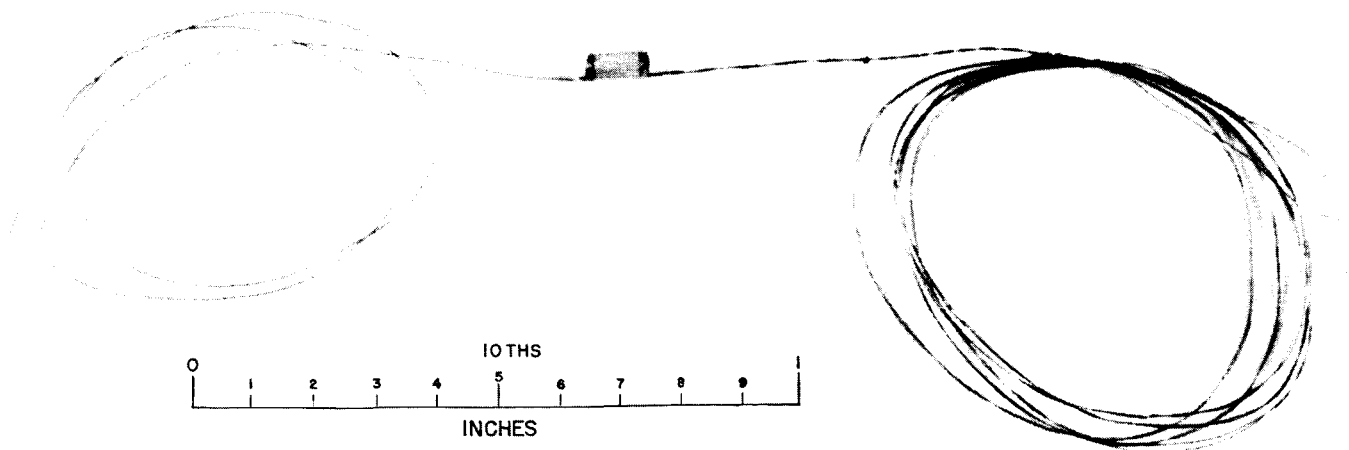


Fig. 4. The miniature stress transducer

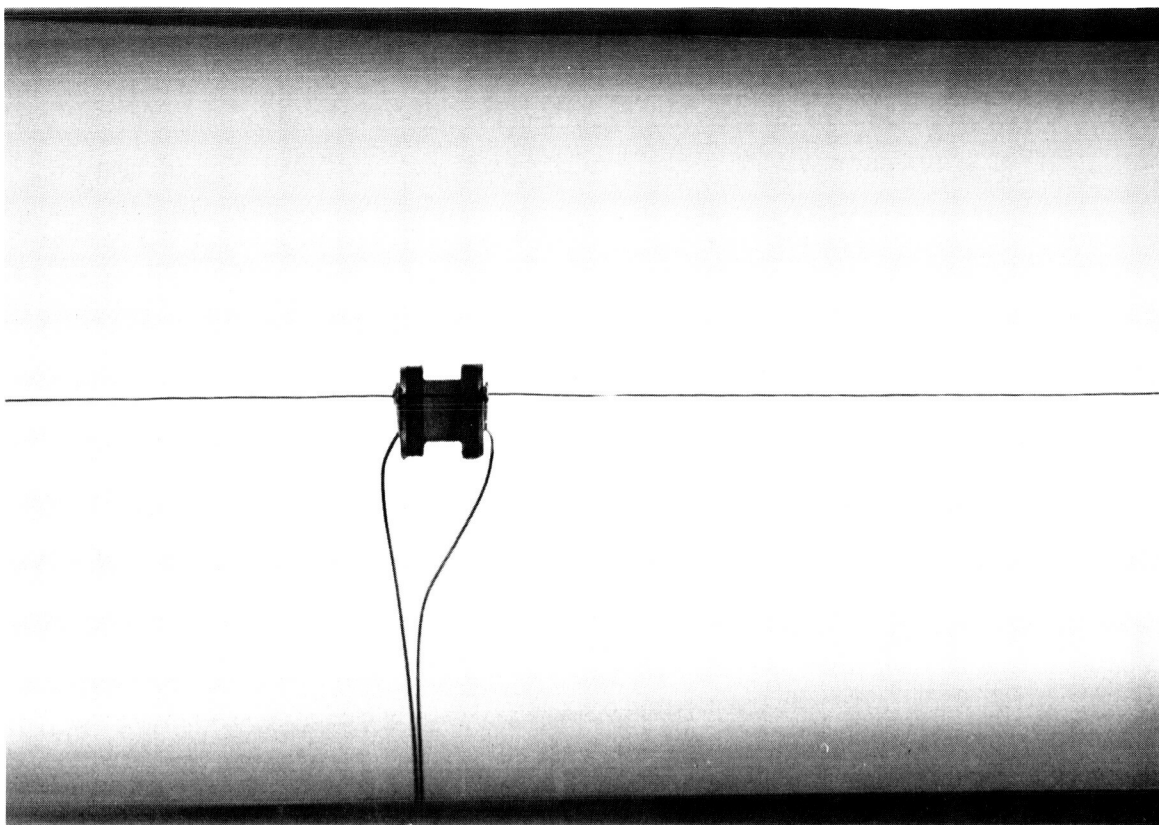


Fig. 5. A spool-type stress transducer in a tensile bar

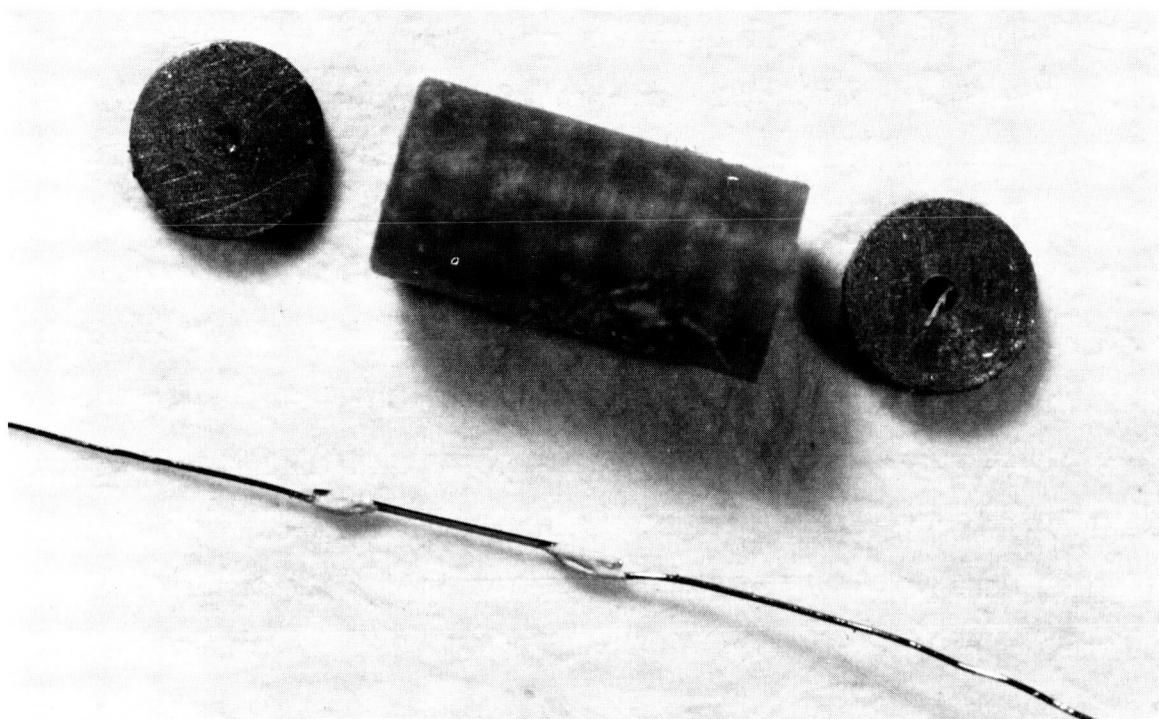


Fig. 6. Basic elements of the miniature stress transducer

since the piezoresistance response of the silicon splinter (because of its orientation) isolates *total* force in only one predetermined direction, which is a function of the crystallographic orientation initially chosen for the silicon splinter, e.g., lateral loads may induce lateral strains but not effect a change in over-all resistance.

By positioning three transducers in three principal orthogonal directions, the total force in the three directions may be isolated and measured (Fig. 7). The forces can be generated only by the surrounding medium (matched boundary conditions). Hence, three-dimensional forces (stresses) can be measured in a point region. These

forces are directly related, through mechanical properties, to the environment being imposed upon the propellant under investigation. The question regarding the effect of the transducer on the surrounding material is moot, since the transducer itself should be thought of as a common force-reaction point. As in all structural problems, it is recognized that stress concentrations exist in the neighborhood of physical force action and reaction points. However, if the force point regions are small compared with the structure under investigation (especially in a homogeneous field), it becomes obvious that the problem reduces to that of simple statics where the St. Venant principle can be employed at some moderate

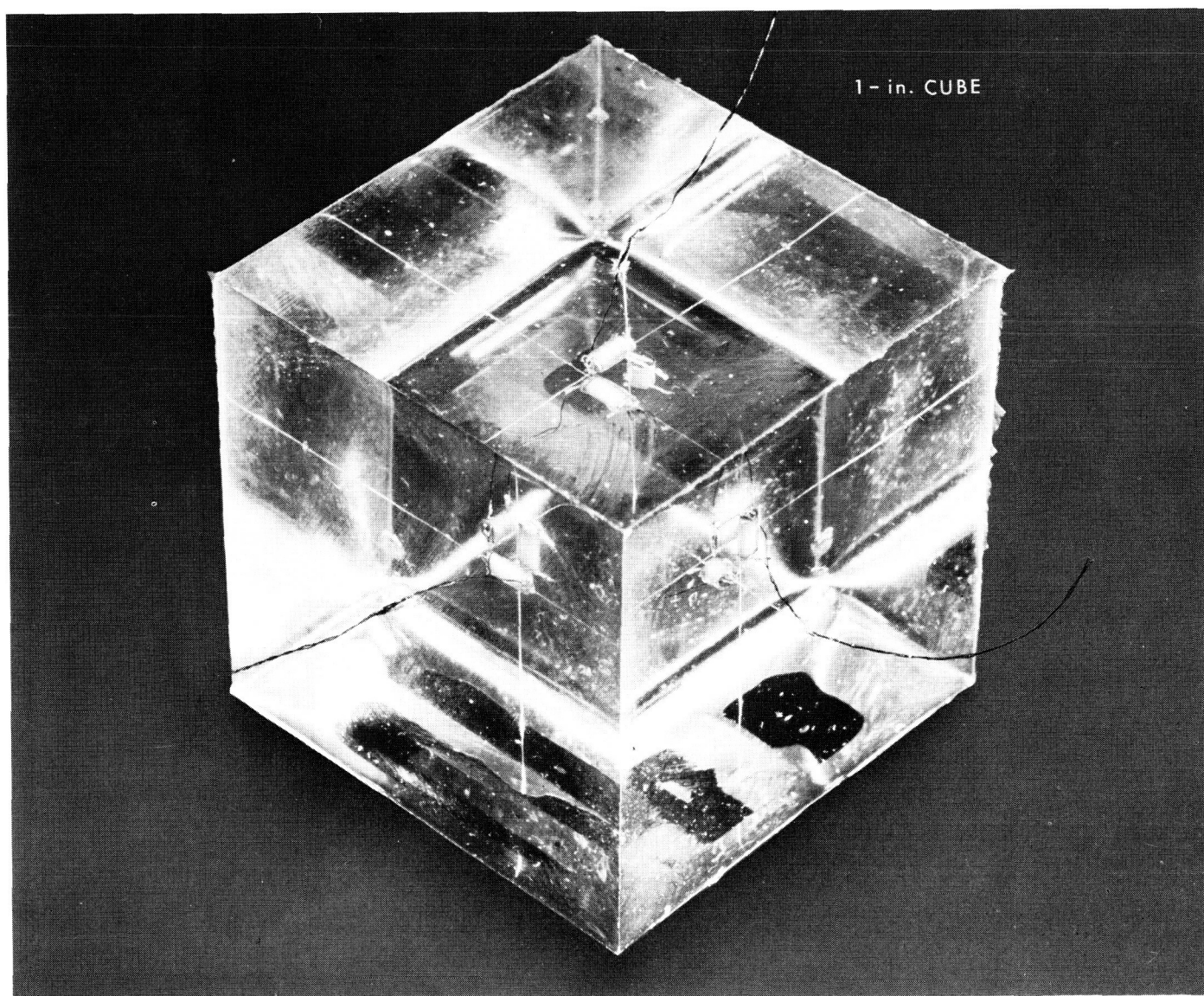


Fig. 7. A preliminary miniature stress rosette

distance away from the transducer. The discrepancy between the stress field near the transducer and the realm where St. Venant's principle is applied can be accounted for by use of an appropriate stress concentration factor, which presumably is only a function of geometry and may be obtained via photoelasticity.

The current construction procedures for the miniature stress transducer follow (Fig. 8): A rod of centerless ground Teflon or other suitable packaging material (0.046-in. D and 0.080-in. length) is drilled out (Fig. 9) along its longitudinal center with a 0.007-in.-D drill. Two end plates are punched out of 0.005-in.-thick stainless steel sheet stock by means of a stamping die. These plates are also drilled out with a 0.007-in.-D drill. Two-mil wire loops and lead wires (Sigmund Cohn, Inc., N.Y.) are then resistance-welded to the end plates. The Teflon rod and end plates are then placed in an ultrasonic cleaner for 30 sec, removed, rinsed in clean acetone, and oven-dried. The Teflon cylinder is next immersed in a Teflon etchant (Bondaidd Etchant, C. H. Biggs, Santa Monica, Calif.) so as to provide an external surface suitable for bonding. An epoxy adhesive (Epon 828/curing agent A, Shell Chemical Co., New York, N.Y.) is then used to bond the end plates to the ends of the Teflon cylinder. The entire assembly is then oven-cured for 2 hr at 200°F. A silicon splinter (Micro Systems, Inc., Pasadena, Calif., Part No. P01-05-120) is then carefully threaded through the cylinder assembly, and gold lead wires are resistance-welded

to each end plate (Fig. 10). A small amount of catalyzed epoxy (Epon 828/curing agent A: 4-8 PPH by wt) is then dipped into the space between the splinter and cylinder cavity by means of a toothpick. Capillary action deposits adhesive into the space between the splinter and cylinder. The assembly is again oven-cured for 2 hr at 200°F. After cure, the transducer is dipped into catalyzed epoxy (Epon 828/curing agent A) and cured according to the previous schedule, while rotating slowly about its transverse axis. The transducer is now complete and ready for the precalibration resistance checkout.

The calibration procedure is to mount the transducer in either a compression block mold (Fig. 11) or a tensile mold (Fig. 12). These molds are then filled with a low-modulus polyurethane resin. The curing schedule for the resin is reported in Ref. 6.

Three calibration runs, measuring the transducer's sensitivity vs. engineering compressive stress, are shown in Fig. 13. These data were obtained by embedding the transducer in an unfilled polyurethane cube (2 in. \times 2 in. \times 2 in.) and applying a uniform compressive load, using greased end plates (Fig. 14). These data demonstrate the reproducibility of the transducer in compression. Similarly, in Fig. 15 are shown tensile stress data for transducers of the same basic design. These latter data were obtained for a transducer embedded in a tensile bar 1 in. in diameter and 5 in. long. An interesting observation of tensile failure is shown in Fig. 16. This particular failure was typical and occurred about $\frac{1}{8}$ in. above the transducer. It was observed that failure initiated at the center of the tensile specimen, as would have been expected. The data points discussed above were obtained from a tension tester load chart and a Speedomax millivolt voltage recorder chart. These data were obtained for a reasonably constant stress rate (0.4 psi/sec).

In order to check for time dependence of calibration curves such as those shown in Figs. 13 and 15, tests can be run at various loading rates. (For the apparatus and strains employed here, a constant strain rate corresponds to a constant stress rate.) Figure 17 shows load vs. time and transducer output vs. time for the various loading rates as indicated. At any given rate, both the load and the output vary linearly with time. The load-output or calibration curve is also linear. However, the slope of the calibration curve will depend on the loading rate, as can be seen by connecting points on the transducer output curve corresponding to given load values (dotted lines). So long as the transducer output is independent of the loading rate, these lines should be horizontal. For the transducer shown, this is true only for stress rates of less than about 2 psi/sec. For higher rates, a single calibration

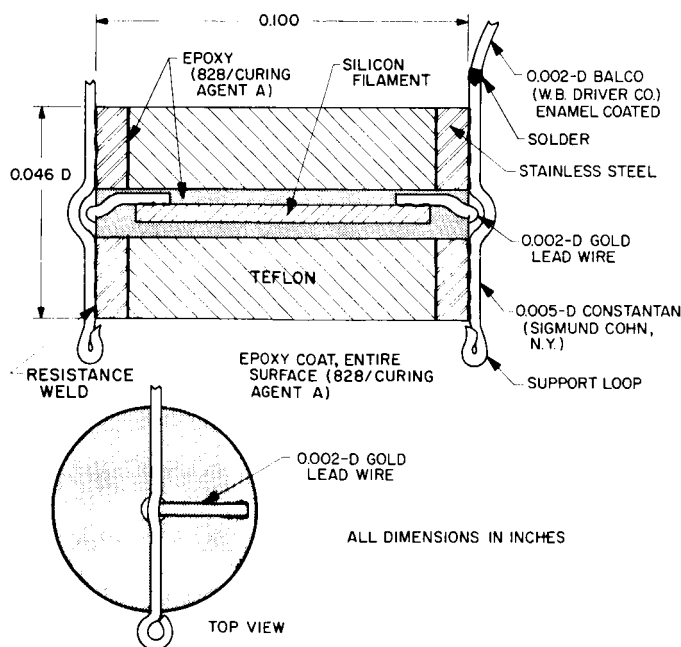


Fig. 8. The construction aspects of the miniature stress transducer

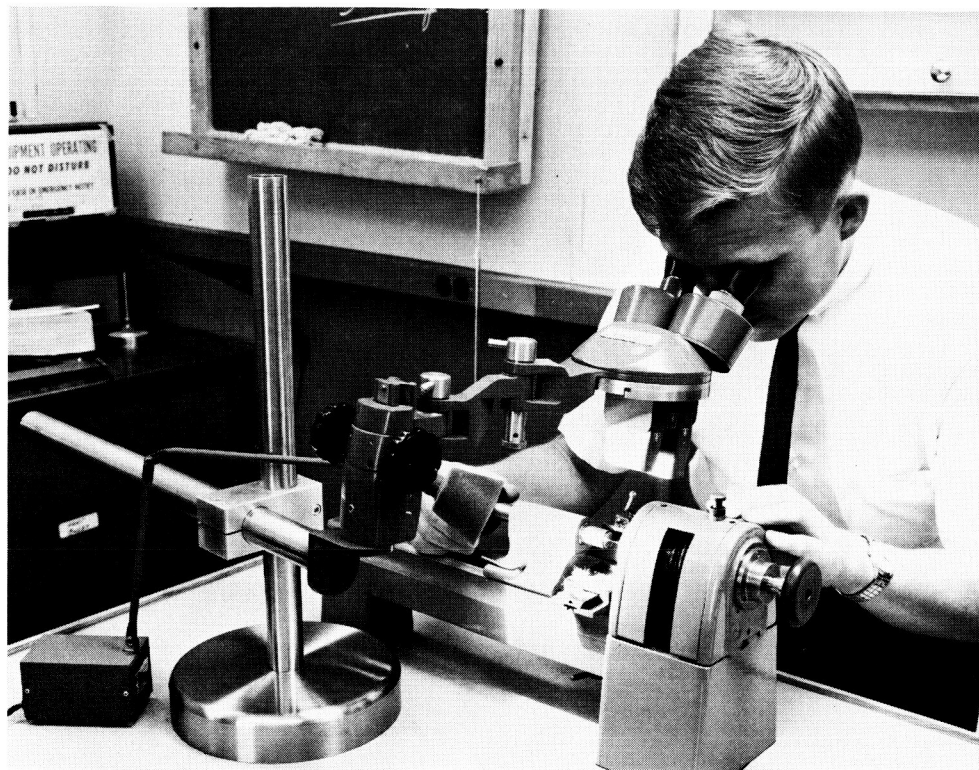


Fig. 9. Jeweler's lathe and magnifying lenses essential to transducer construction



Fig. 10. Threading and welding phase of transducer construction

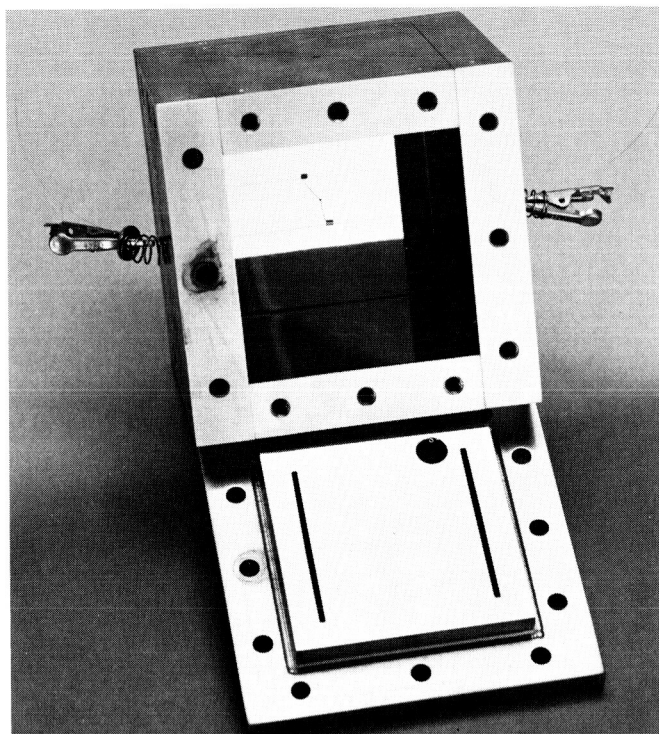


Fig. 11. Compression calibration mold

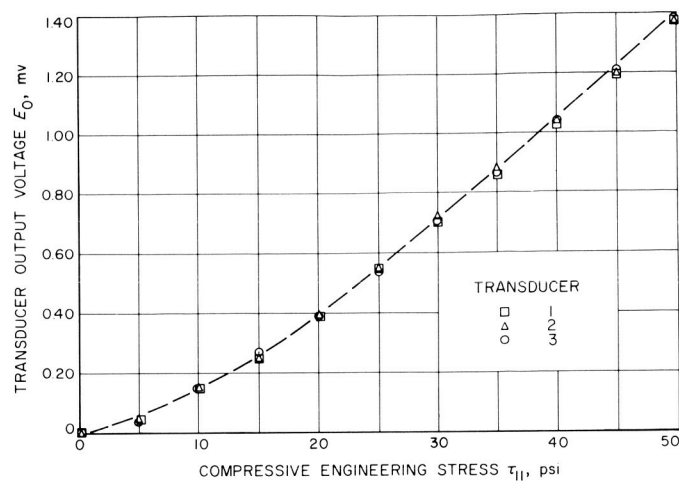


Fig. 13. Calibrated response of transducer in compression

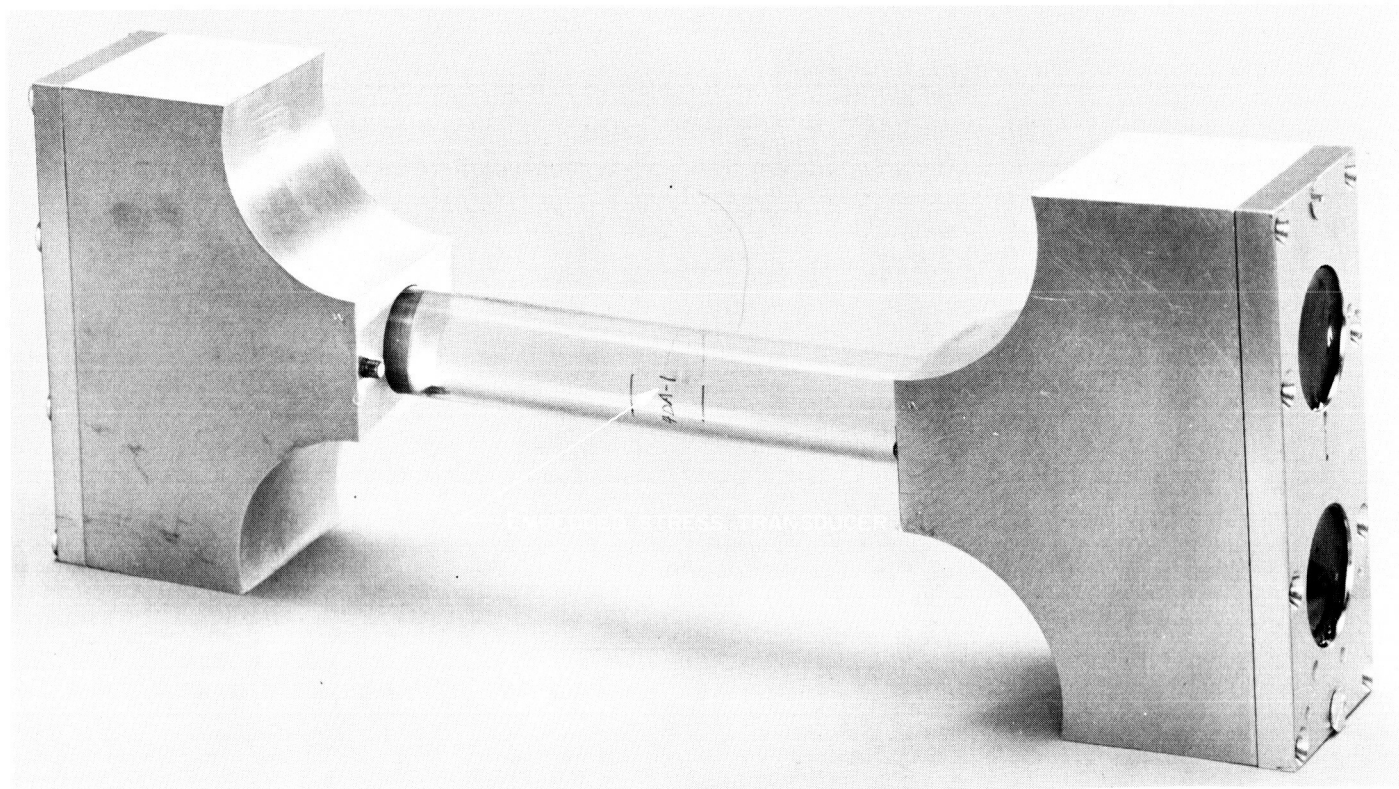


Fig. 12. Tensile calibration mold

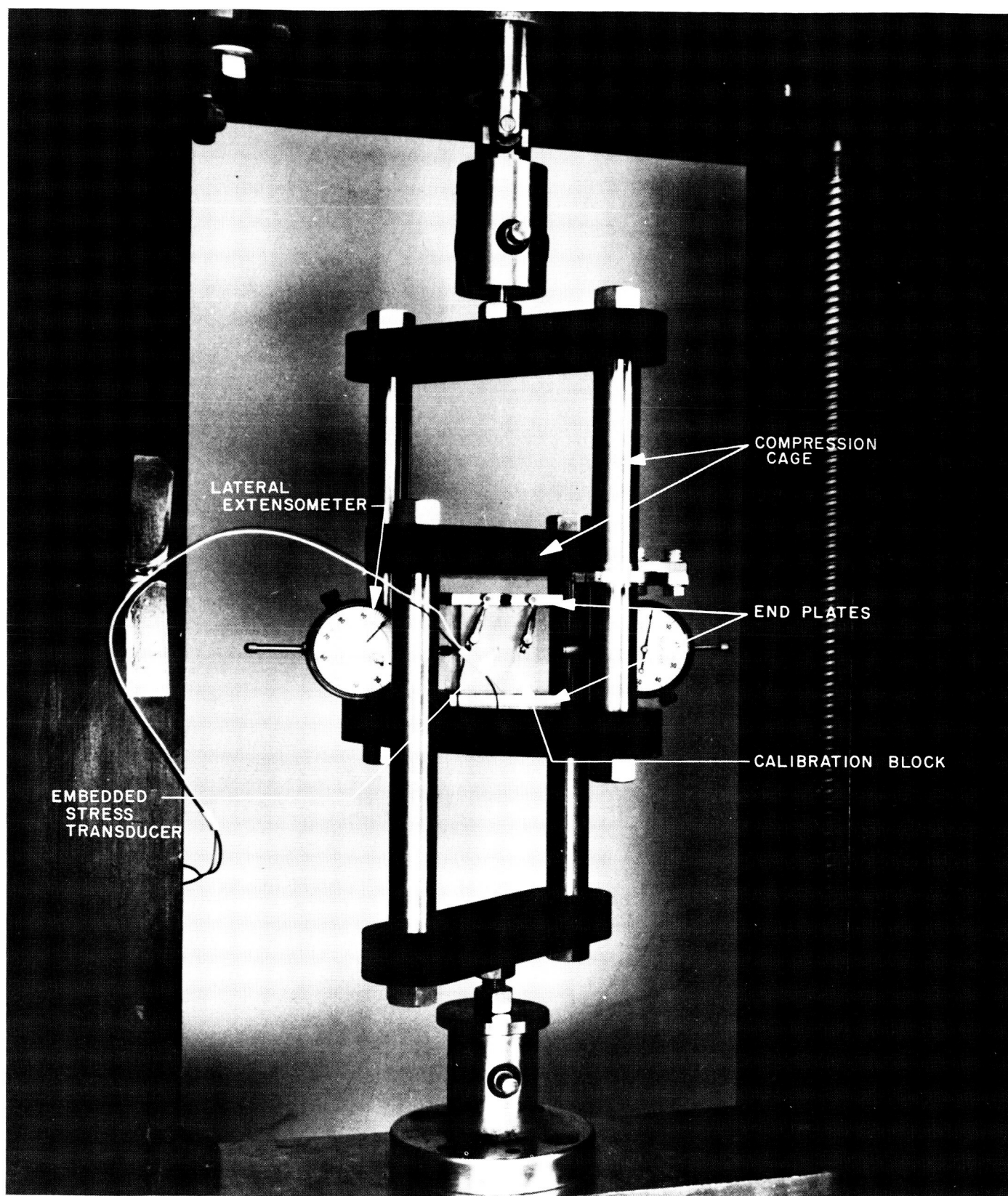


Fig. 14. Compression calibration apparatus

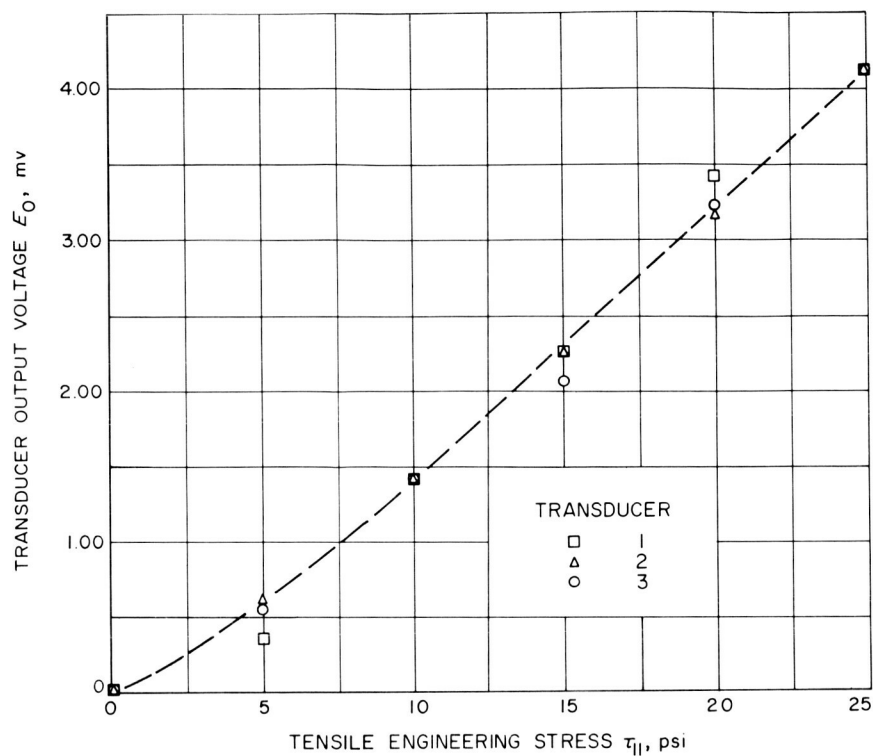


Fig. 15. Calibrated response of transducer in tension

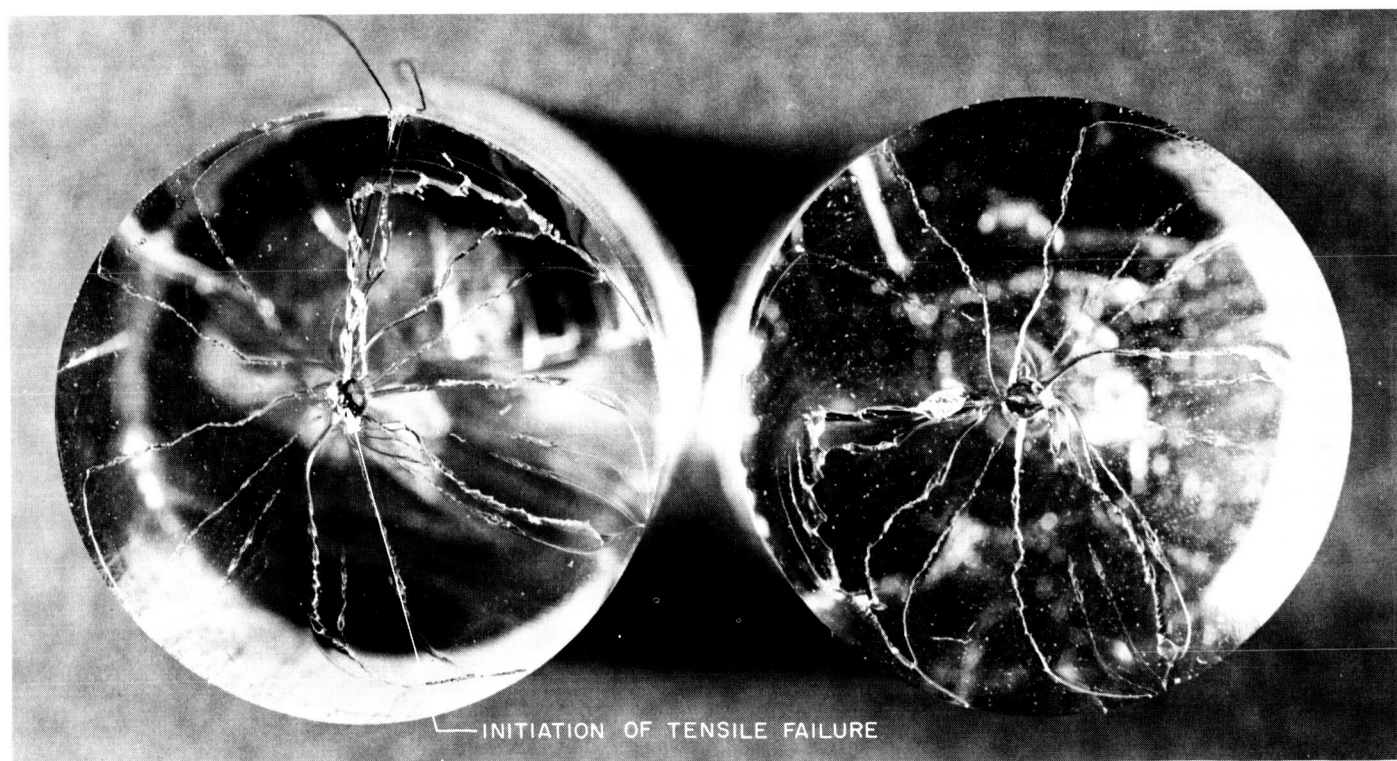


Fig. 16. Tensile failure near the miniature stress transducer

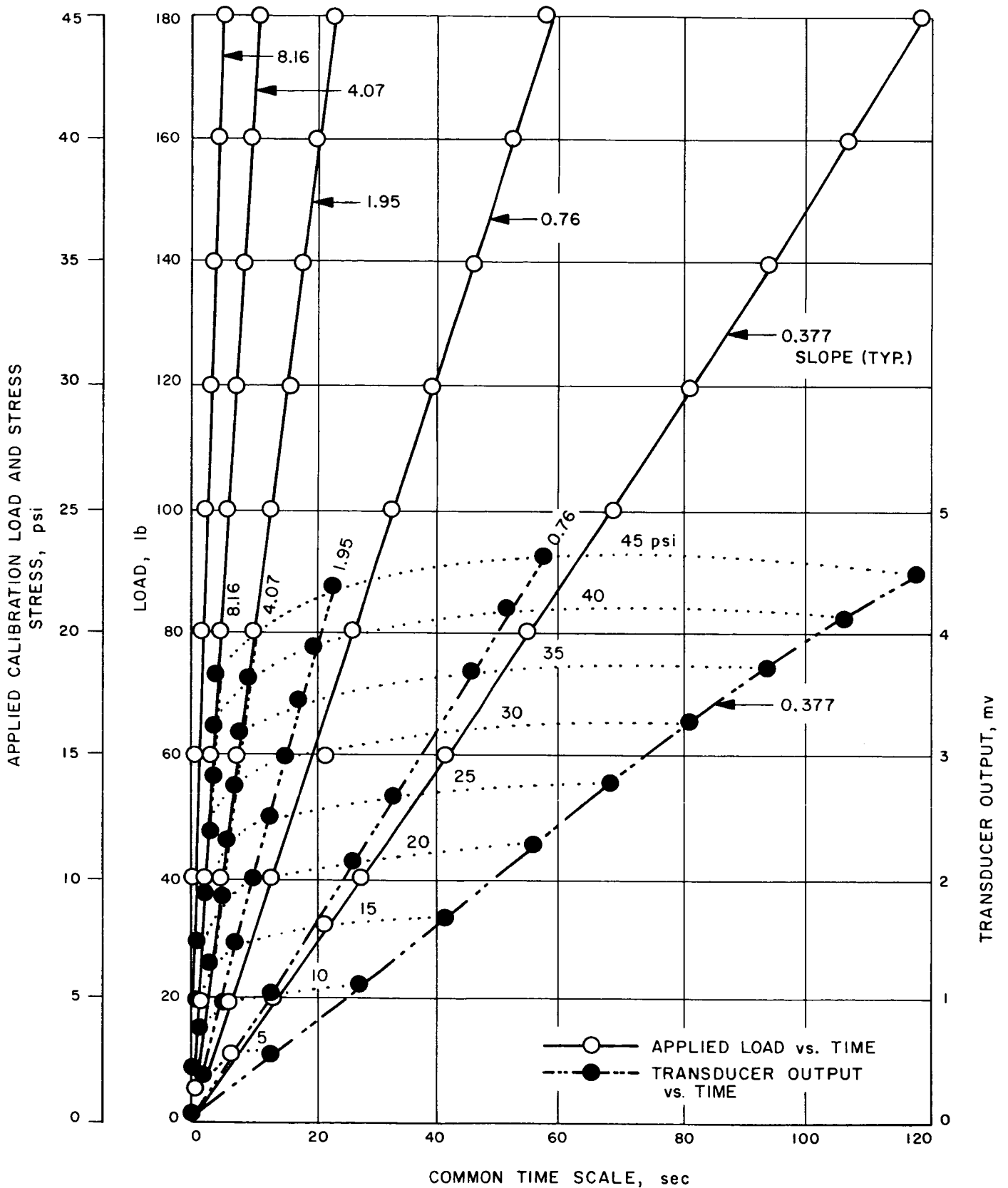


Fig. 17. Stress-rate response of typical transducer

curve is no longer applicable, and the curve applicable to a given loading rate must be used.

Upon completion of the various calibration tests, the miniature stress transducer is removed from the calibration block with acetone. The gage is now ready for casting in a propellant motor.

The observations discussed in this section demonstrate that the voltage output response (for a particular environment and loading rate) of the miniature stress transducer is reproducible and relatively linear when subjected to applied compressive or tensile stress. Therefore, it is suggested that the described transducer is a potential tool for structural design and physical property studies.

IV. GAGE APPLICATION

One application of the stress transducer described above is to measure the radial stress (actually the total force in the radial direction) at a point region within the interior of a thick-walled, unfilled polyurethane cylinder. The fixture used to mount the transducer was a polished mold 6 in. in diameter and 6 in. in length, using a mandrel (Fig. 18). The transducer could then be mounted within the mold in a predetermined position prior to casting a mixture of Solithane 113 prepolymer and castor oil into

the mold. Greased lead wires (2.5 mil in diameter) were inserted to record the transducer's resistance change due to the radial stress. These extended to and from the transducer through the same greased tunnel (5 mil in diameter) in the polyurethane cylinder and mold wall. A removable wire was positioned between the transducer and the two sides of the cylindrical mold (Fig. 19). This wire was used for mounting purposes only and was housed in a greased tunnel for easy removal. The thick-walled cylinder with embedded transducer was then subjected to the inflated cylinder test (Fig. 20).

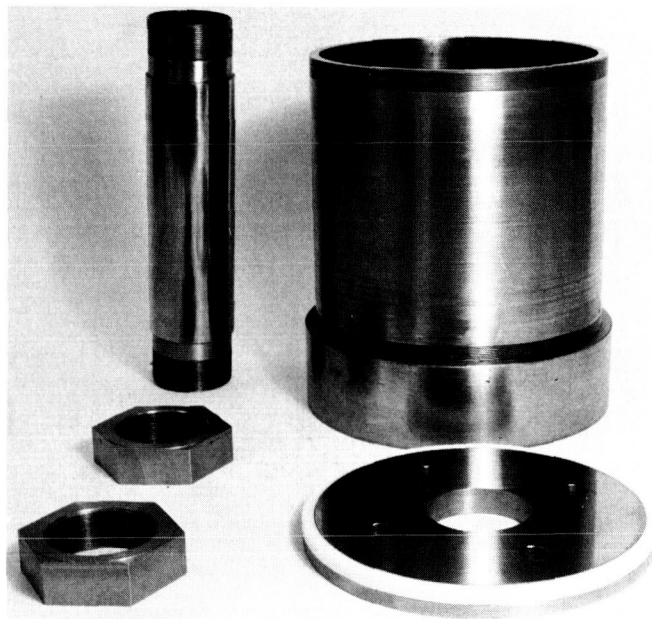


Fig. 18. Transducer-positioning mold

The inflated cylinder test consists of pressurizing a greased rubber bag within the cavity of an unrestricted thick-walled cylinder. The bag is longitudinally retained within the cavity by two end plates, which are monitored by a servo system that insures bag containment yet does not allow any consequential longitudinal load to exist in the thick-walled cylinder.

An arbitrary pressure schedule (less than 2 psi/sec) was selected to insure that rate effects would not affect the transducer output or cause the cylinder response to deviate extremely from the quasi-elasticity assumption prerequisite for the classical cylinder equations. Three transducers of similar design (but differing sensitivity) were calibrated in a rectangular stress field. The transducers were then recovered from the calibration blocks and embedded in three separate polyurethane cylinders. Internal bag pressure was increased until complete failure of the thick-walled cylinder was accomplished.

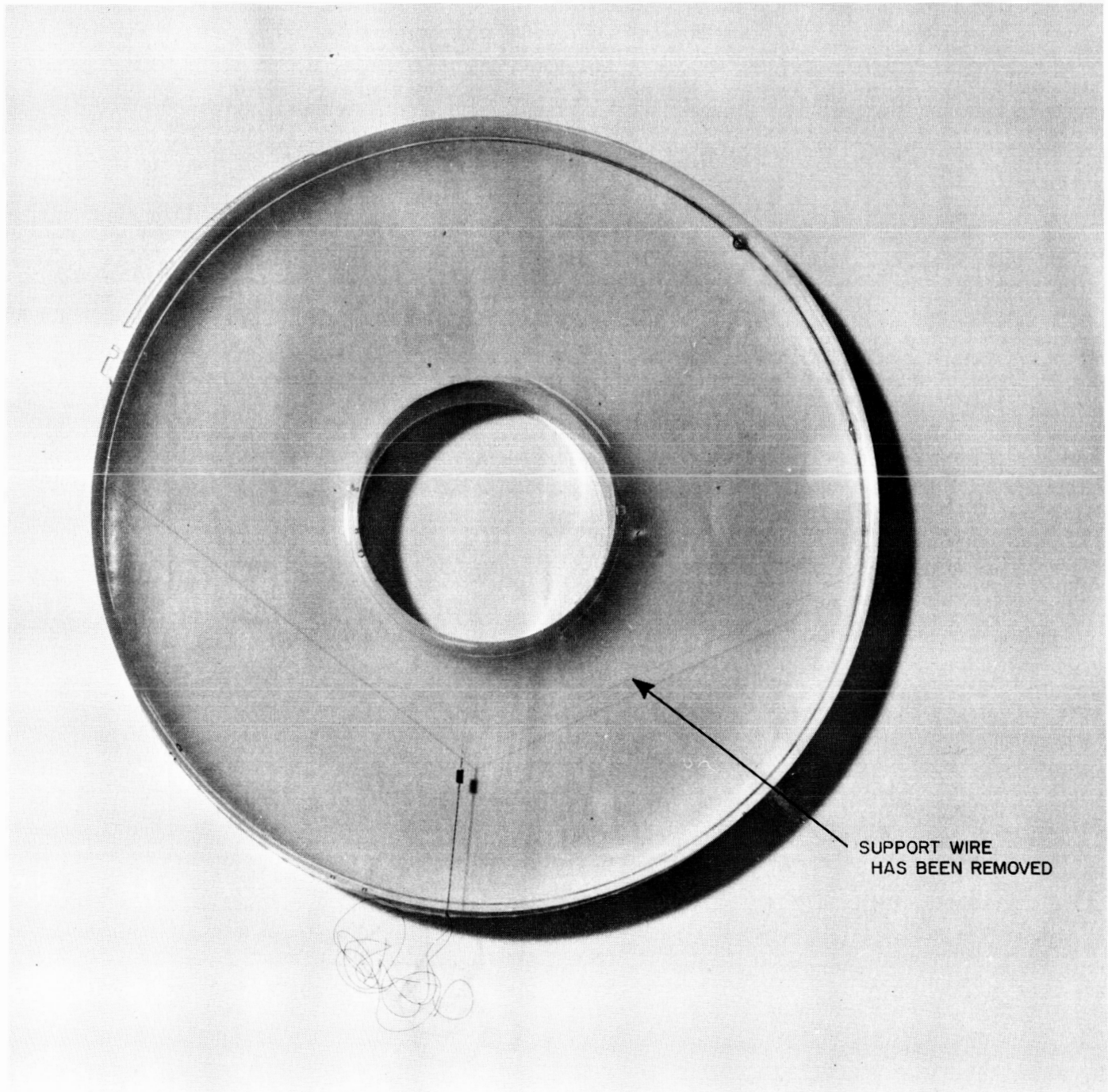


Fig. 19. Positioned transducer in thick-walled cylinder

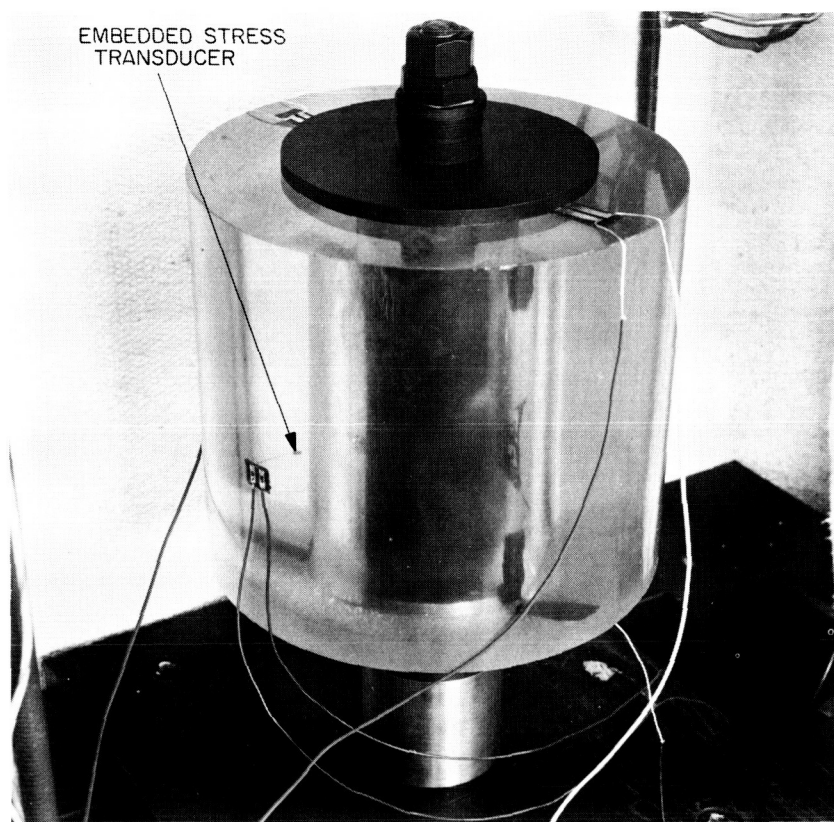


Fig. 20. Inflated cylinder test

V. DISCUSSION

The three separate transducer outputs are shown in Fig. 21. Also shown in this figure is the theoretical value of radial compressive stress. As expected, the transducer's response obviously indicates a stress level greater than that predicted by theory.

An explanation for the discrepancy between the transducer response and the theoretical estimate is that a stress concentration exists between the transducer and the surrounding polyurethane rubber. A stress concentration factor of about 1.7 would account for the discrepancy between theory (without inclusion) and experiment (with inclusion).¹ In principle, the stress concentration factor should be incorporated in the calibration factor, but it is not, in the present instance, because the transducer

was calibrated while embedded in a cube calibration block, although it was used in a polar-coordinate deformed cylinder. In any event, this stress concentration effect is not considered serious, because steps can be taken via photoelastic stress freezing to eliminate the major source of the stress riser. In this manner, the transducer can be redesigned on a trial-and-error basis.

However, it would be premature to write off the discrepancy between theory and experiment to a stress concentration factor. Other factors may be contributing significantly to the discrepancy, the most significant being the fact that the theoretical prediction is based on linear theory and an infinitely long cylinder (note that material properties do not enter into the cylinder equations). A relatively low-modulus material was used for the test cylinders in this Report, in order that the stress measure-

¹Note: In general, a stress concentration factor is assumed (via photoelasticity) to be independent of the magnitude of the stress field.

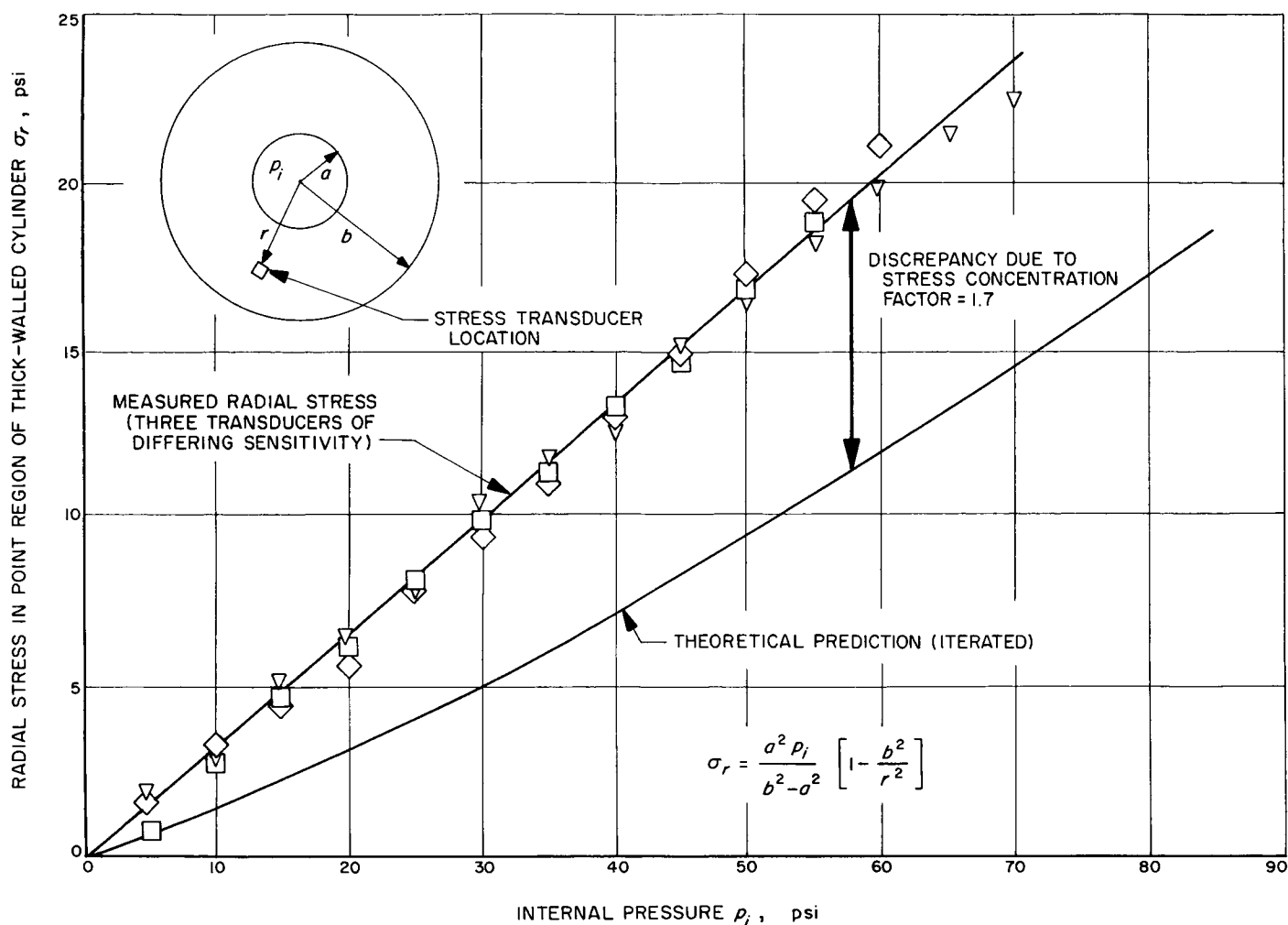


Fig. 21. Experimental vs. theoretical values for radial stress in a pressurized cylinder

ments would be in the large-strain realm representative of a solid propellant grain. Consequently, an iterative solution was developed by replacing the value of the "constants" a and b for each pressure level in the linear cylinder equation (Fig. 21). This iterative process caused the curving of the "theoretical prediction of stress" curve toward the measured-stress curve in Fig. 21. The extent of the discrepancy introduced by this approximation is

not clear. However, these and related questions are for future study.

Another point of interest is that three independent transducers of differing sensitivity measured approximately the same radial stress. This observation shows that the entire scheme has reasonable repeatability as well as validity.

VI. CONCLUSION

A stress transducer has been constructed to measure, with suitable calibration corrections, the radial stress within a thick-walled cylinder of polyurethane. The transducer is also applicable for solid-propellant stress measurements.

NOMENCLATURE

E_i	electric field components of silicon splinter
i_i	current components of silicon splinter
l_{ij}	direction cosines associated with the crystallographic axis of the silicon splinter
R_0	resistance of silicon splinter
R_i	resistance of Wheatstone bridge arms
$\pi_{11}, \pi_{12}, \pi_{44}$	piezoresistive electromechanical coupling coefficients unique to silicon
ρ	resistivity, ohm-cm
τ_{ij}	principal stress tensor acting on silicon splinter

REFERENCES

1. Durelli, A. J., *Survey of Strain Measuring Methods*, Aerojet-General Corporation, Report No. 0411-10F, Contract AF33(600)-40315, Appendix B, March 1962.
2. Dicken, G. M., and Thacher, J. H., "Shear Strain Measurement in Solid-Propellant Rocket Motors," presented at the American Institute of Aeronautics and Astronautics meeting, Washington, D. C., June 28-July 2, 1964.
3. Schwartz, D. S., *Development of Unidirectional D.C. Axial and Radial Flexible Propellant Shear Strain Transducers*, Gulton Industries, Inc., Final Report to Hercules Powder Company, Purchase Order No. ABL-73197, November 1963.
4. Silver, R. H., and San Miguel, A., "Preliminary Studies of a Miniature Stress Transducer, I," *Quarterly Summary Report No. 38-12*, Jet Propulsion Laboratory, Pasadena, Calif., July 31, 1963, pp. 26-31. CONFIDENTIAL.
5. Phann, W. G., and Thurston, R. N., "Semiconducting Stress Transducers Utilizing the Transverse and Shear Piezoresistance Effects," *Journal of Applied Physics*, Vol. 32, No. 10, October 1961, pp. 2008-2019.
6. San Miguel, A., and Duran, E. N., "Some Low-Modulus Birefringent Resins," *Experimental Mechanics*, Vol. 4, No. 3, 1964, pp. 84-88.
7. San Miguel, A., and Silver, R. H., *A Normal-Incidence Reflective Polariscope for Viscoelasticity Measurements*, Technical Report No. 32-573, Jet Propulsion Laboratory, Pasadena, Calif., June 1, 1964. (Presented to the Society for Experimental Stress Analysis, May 7, 1964.)
8. *Semiconductor Strain Gages*, ed. by M. Dean, Academic Press, New York, 1962.
9. Mason, W. P., and Thurston, R. N., "Use of Piezoresistive Materials in the Measurement of Displacement, Force, and Torque," *Journal of the Acoustical Society of America*, Vol. 29, No. 10, October 1957, pp. 1096-1101.

ACKNOWLEDGMENT

The authors wish to acknowledge the advice and technical support of V. H. Culler, E. N. Duran, R. F. Landel, and A. Merko.